Giant Smooth Muscle Cells of *Beroë*

Ultrastructure, Innervation, and Electrical Properties

M-L. HERNANDEZ-NICAISE, G. O. MACKIE, and R. W. MEECH

From the Laboratoire d'Histologie et Biologie Tissulaire, Université Claude Bernard-Lyon I, Villeurbanne, France; the Biology Department, University of Victoria, Victoria, British Columbia, Canada; and the Department of Zoology, University of Cambridge, Cambridge, England. Dr. Meech's present address is Department of Physiology, University of Utah Research Park, Salt Lake City, Utah 84108.

ABSTRACT *Beroë* muscle fibers are single cells which may be 20–40 μm in diameter in mature specimens. Longitudinal muscles may be 6 cm or more long. There is no striation pattern and the muscles were observed to contract in a tonic fashion when stretched. They are innervated by a nerve net, and external recording revealed what are probably nerve net impulses. Intracellular stimulation of the muscles themselves was found to initiate large propagating action potentials which were recorded intracellularly. The action potentials were insensitive to tetrodotoxin (10^{-5} g/ml), tetraethylammonium ions (50 mM), $MnCl_2$ (25 mM), and low concentrations of verapamil (2×10^{-6} g/ml). Full-size action potentials were recorded in sodium- or calcium-deficient salines, but were small and graded in salines deficient in both sodium and calcium. Cable analysis yielded mean values for λ(1.95 mm), R_i (154 Ωcm), R_m (9,253 Ωcm^2), and τ_m (13.9 ms). The conduction velocity depended primarily on fiber diameter and maximum rate of rise of the action potential and could be predicted from the theoretical analysis of Hunter et al. (1975 *Prog. Biophys. Mol. Biol.* **30:** 99–144). The calculated membrane capacity (<2 μF/cm^2) indicates little infolding of the surface membrane, a conclusion which is in agreement with anatomical studies.

INTRODUCTION

Beroid ctenophores possess a system of mesogleal muscle fibers organized into several distinct fields and innervated by processes of the ectodermal nerve net (Hertwig, 1880; Franc, 1970; Hernandez-Nicaise, 1973 *a,b,c*). Each muscle fiber is a single cell that appears to contract in a tonic fashion when stretched and displays no striation pattern. This together with other criteria suggest that the fibers may be classified as smooth muscle. They run independently for considerable distances (6 cm or more) and are large enough (20–40 μm in diameter) to permit intracellular recording. Intracellular stimulation initiates large propagating action potentials without noticeably shortening the muscle.

J. GEN. PHYSIOL. © The Rockefeller University Press · 0022-1295/80/01/0079/27 $1.00 79
Volume 75 January 1980 79–105

This paper gives the results of a study of these muscle cells in specimens of *Beroë ovata*. It includes (*a*) a preliminary investigation of their cable properties, (*b*) a description of the ionic basis of the action potential, (*c*) extracellular recordings from epithelial surfaces of the body wall, and (*d*) an account of the histology of the body wall to provide a structural background for these results. We know of no previously published records of electrical activity recorded either intracellularly or extracellularly from any ctenophore, a phylum which occupies an isolated position in the invertebrata.

MATERIALS AND METHODS

Specimens of *Beroë ovata* (Fig. 1 *a*) were collected at the Station Zoologique, Université Pierre et Marie Curie, Villefranche-sur-Mer, France. They were kept in seawater at 10°C prior to the experiments, but all experiments were carried out at room temperature 20–22°C.

Electron Microscopy

Whole animals were fixed in 3% glutaraldehyde in cacodylate-buffered (pH 7.5) saline (composition in millimolar: 100 Na cacodylate/HCl, 400 NaCl, 10 KCl, 10 $CaCl_2$, 58

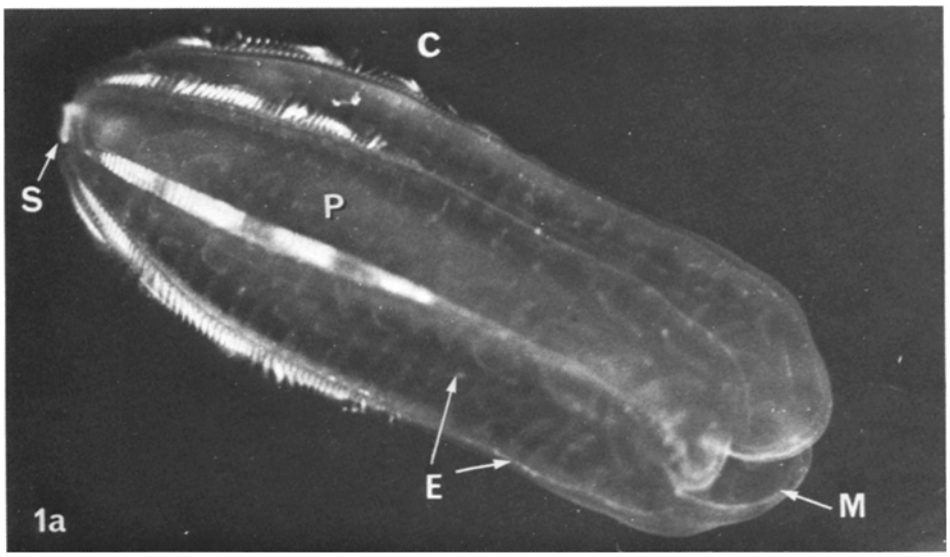

FIGURE 1. (*a*) Photograph of an adult *Beroë ovata* swimming freely. The whitish central zone corresponds to the flattened pharynx (P). The bulk of the body is made up by a transparent nonfibrous matrix, the mesoglea, through which run endodermic channels (E). (M) Mouth leading to pharynx; (C) ciliated comb plates, the locomotory organs of the animal; (S) aboral sensory organ. (*b*) Diagram of the muscular system of *Beroë ovata*. The body wall has been sectioned perpendicularly to the longitudinal axis of the animal. Nerve cells and neurites are shown in black, mesoglea is dotted, and nuclei are striped. (ELM) External longitudinal muscles; (PCM) pharyngeal circular mesogleal muscles; (PLE) pharyngeal longitudinal subepithelial muscles; (RM) radial muscles. The diagram gives a general idea of the relationship between different tissues. For sake of simplicity only one layer of longitudinal fibers is represented, and the diameter of muscle fibers is not exactly to scale.

$MgCl_2$). They were then briefly rinsed in buffered saline. Small pieces were dissected out and postfixed in the same saline containing 1% osmium tetroxide, prior to embedding in Epon (Shell Chemical Co., New York). Sections were stained in uranyl acetate and lead citrate and were examined with a Philips EM300 (Philips Electronic,

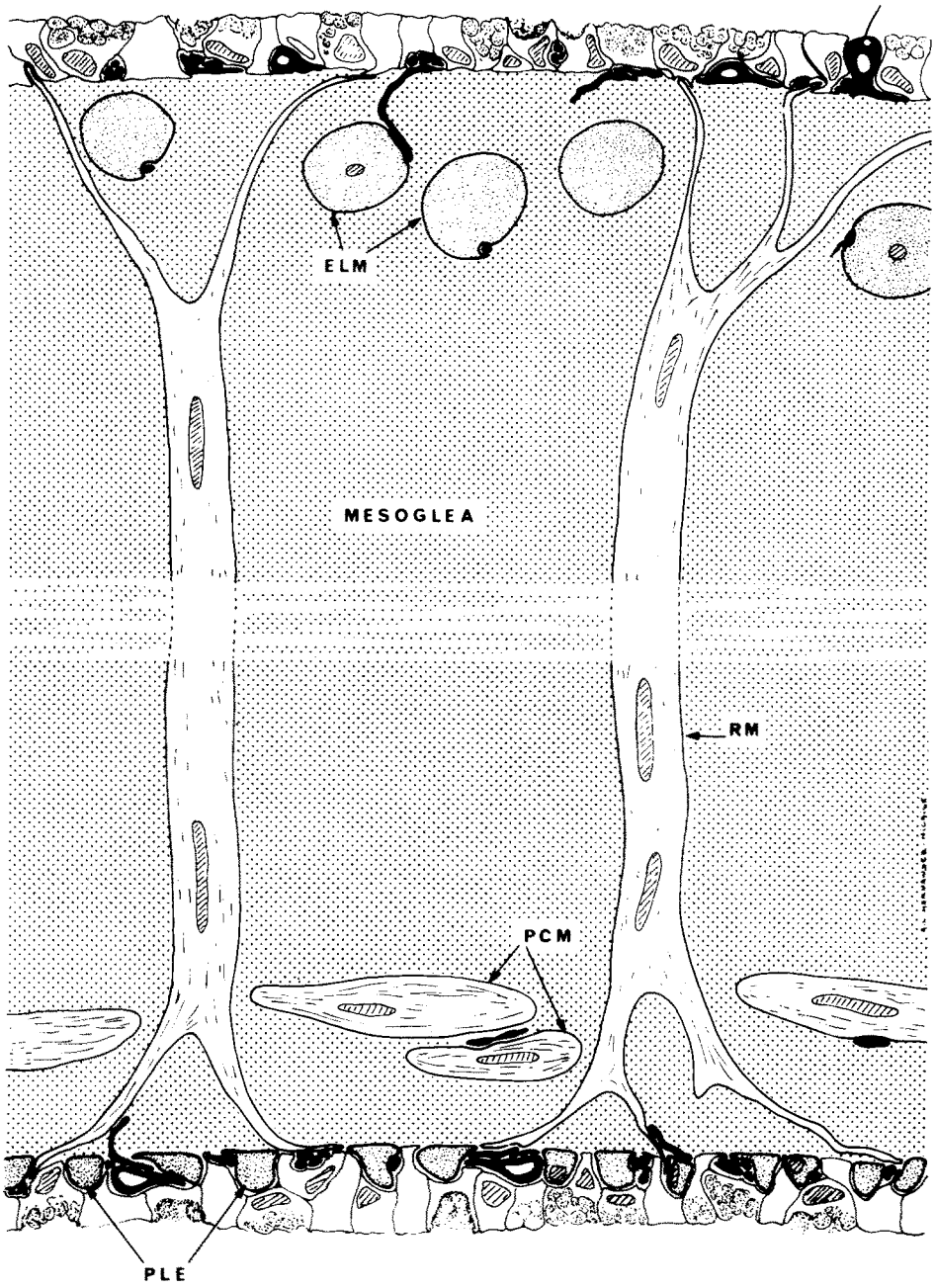

1b

Mahwah, N.J.) or a Hitachi 12A (Hitachi Ltd., Tokyo) electron microscope at the Centre de Microscopie Électronique Appliquée á la Biologie et la Géologie, Université Claude Bernard.

Electrophysiology

Extracellular recordings from the surface of the body wall of whole animals were made with fine polyethylene suction electrodes connected to high-gain, differential, AC amplifiers (Tektronix, Inc., Beaverton, Ore., model 5A22N) and a storage oscilloscope. Stimuli were delivered through similar electrodes.

In order to stabilize the preparation for work on individual muscle fibers, a core of tissue was dissected from the body wall and sucked into a translucent plastic tube (diameter 6 mm). The tissue was bathed in artificial seawater having the following composition in millimolar: 500 NaCl, 10 KCl, 11 $CaCl_2$, 58 $MgCl_2$, 50 Tris/Tris-HCl at pH 7.5. Muscle fibers embedded in mesoglea were visible through a hole in the side of the tube, which was illuminated from below. Individual fibers could be traced for distances of up to 5 mm. However, fibers that had been cut during the dissection appeared to reseal, and even quite short lengths of fiber (1–2 mm) were found to be excitable. Consequently, shortened lengths of fiber (1–6 mm) were used for most of the experiments. The muscle fibers were difficult to penetrate because they were displaced by the micropipette as it passed through the mesoglea. If the mesoglea was digested with hyaluronidase (hyaluronidase type II, 0.25 mg/ml, Sigma Chemical Co., St. Louis, Mo.) for 15–30 min, it became possible to penetrate single fibers with two or more 3 M KCl-filled micropipettes. Each micropipette had a resistance of 30–100 MΩ and a tip potential of <5 mV. One or more micropipettes were used to record the membrane potential. They were connected to a capacity-compensated unity-gain preamplifier and a storage oscilloscope. Another micropipette was used to pass current across the fiber membrane. The current passed was measured as the potential across a 10 KΩ resistance to ground.

Although spontaneous action potentials were recorded from these shortened fibers on only two occasions, the tissue as a whole was often spontaneously active. Slow, irregular movements, which originated in the band of circular muscle below the pharyngeal epithelium, invariably dislodged the micropipettes a few minutes after penetration. In an exceptional case, it was possible to hold two micropipettes in a fiber for 30 min. In experiments with verapamil, tetrodotoxin (TTX), cobalt chloride, and manganese chloride, it was possible to record continuously while adding a few drops of the concentrated solution to the bathing medium. However, it was not possible to record while allowing the fibers to recover from such treatment. It was only possible to show that other fibers recovered when the preparation was washed in normal artificial seawater.

RESULTS

Histology and Ultrastructure

The general relationship between the mesogleal muscles is shown in Fig. 1 *b*. Three systems can be recognized, the external longitudinal muscles (ELM), which are just under the epithelium at the outer surface; the radial muscles (RM), which cross the body wall; and the thin pharyngeal circular muscles (PCM), which are seen in longitudinal section in Fig. 1 *b*. The circular muscles form a continuous sheet whereas the radial and longitudinal muscles are well

separated. There are also large longitudinal muscles that run just below the circular muscles, but these are not shown in the figure.

Because of the transparency of the mesoglea and the large size and relative isolation of the muscle cells, a considerable amount of detail can be made out by light microscopy on whole-mount preparations (Figs. 2, 5, and 6). Each mesogleal muscle fiber is a single long cylinder of fairly regular diameter but with occasional swellings or constrictions. The diameter increases with the age and size of the animal and so varies from 5 to 50 μm. In a big, mature specimen the radial fibers are the thickest, usually 20–40 μm in diameter.

The radial muscles branch at both ends, one anchoring on the external covering epithelium and the other on the pharyngeal epithelium (see Fig. 5). The length of a radial fiber is equal to the thickness of the body wall and so varies with the size of the animal, reaching 1 cm in animals 10–15 cm long. The entire length of a radial fiber may be observed under Nomarski interference contrast. No membranous partitions are observed and the myofilaments appear continuous. Each fiber is therefore assumed to be a single cell.

The longitudinal muscles have smooth tapering ends, and both ends are anchored in the same epithelium. They are of variable length and sometimes branch (Fig. 2). Fibers of 6 cm have been isolated by dissecting fixed whole animals. As in the case of the radial muscles, these fibers are assumed to have a continuous cytoplasm because no membrane partitions have been observed in either electron microscope (EM) sections or under Nomarski optics.

An extensive EM survey[1] has shown that the general organization of all mesogleal muscle cells is the same. Numerous nuclei distributed at irregular intervals can be seen in all fibers under light microscopy (Figs. 2 and 5) whereas EM sections show a central cytoplasmic core surrounded by contractile filaments (Fig. 3). The cytoplasmic core contains mitochondria, sacs of smooth and rough endoplasmic reticulum, Golgi bodies, and abundant ribosomes around the nuclei. The thick contractile shaft surrounding the cytoplasm is penetrated by microtubules and by a longitudinal system of tubules of the sarcoplasmic reticulum (Fig. 3).

A preliminary stereometric analysis on 25 transverse sections from different cells (diameter 9–25 μm) showed that the sarcoplasmic reticulum accounts for <1% of the volume of the muscle cell (0.6–2%; mean 0.92%). We have not observed any well-developed system of peripheral contacts between the sarcoplasmic reticulum and the sarcolemma although such an association was found at two discrete locations: at the areas of contact between muscle cells (which are few) and at neuromuscular junctions.

The contractile shaft is made up of thick filaments, 12–20 nm in diameter (mean 11.5 nm) and thin filaments, 5–6.7 nm in diameter (mean 6 nm). The thin filaments are organized in more or less regular rosettes around the thick filaments with a ratio of 1 thick to 5–9 thin (Fig. 4). No striation pattern has been observed nor any dense body or attachment plate. The thin filaments are probably attached to the cell membrane, and this may account for the way in which the muscle seals when damaged.

[1] Hernandez-Nicaise, M-L., and J. Amsellem. Manuscript in preparation.


Mi
2
30 µm

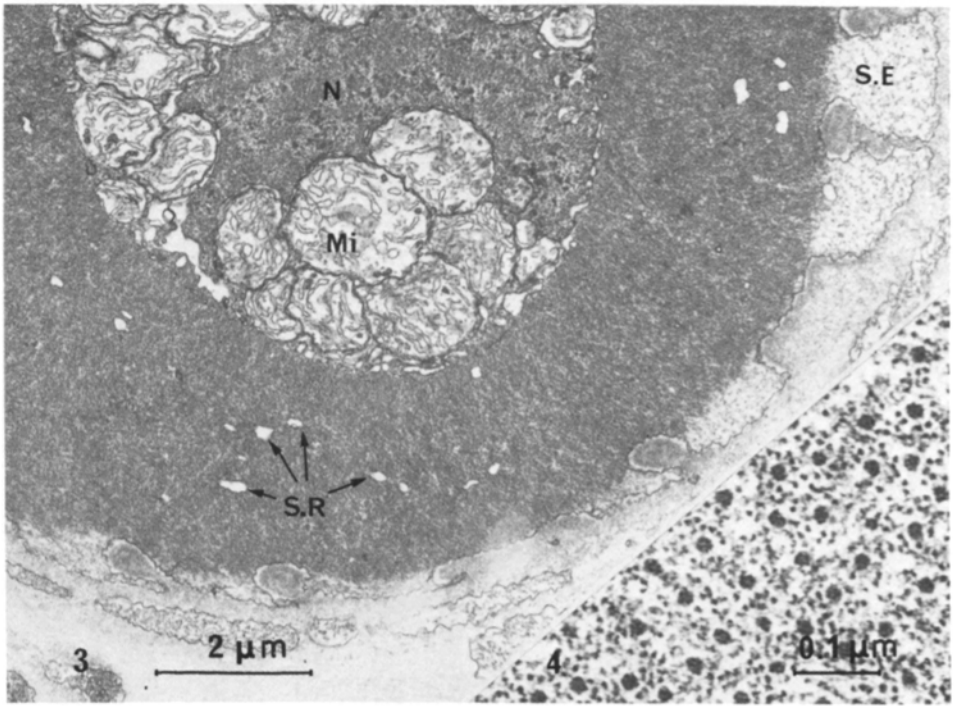
N
S.E
Mi
S.R
3
2 µm
4
0.1 µm

The cell membrane occasionally invaginates, building a loose peripheral system of tubular sacs. Such figures are reminiscent of the *caveolae intracellulares* or surface vesicles described in vertebrate smooth muscle cells (Devine et al., 1972; Gabella, 1973) although in *Beroë* the system is much less developed. In many cross sections the cell periphery shows large evaginations lacking myofilaments (Fig. 3). These can also be seen as finger-like projections under light microscopy (Fig. 5).

Close membrane appositions resembling gap junctions have been observed at points of contact between muscle fibers, but these are few in number and have not been studied in any detail. None of the cells used for the electrophysiological analysis appeared to make contact with any other fiber.

The muscle cells are innervated by the nerve net which underlies the epithelia (Fig. 6). Most of the neuromuscular junctions are found near the epithelia. At the neuromuscular junction (Fig. 7) the neurite contains one or several "presynaptic triads" (synaptic vesicles-endoplasmic reticulum-mitochondrion) as in interneuronal synapses (Hernandez-Nicaise, 1973 *c*). To judge from the high frequency of synapses encountered in EM sections, it seems probable that each intramesogleal muscle cell is individually innervated. There is evidence that the longitudinal muscles under the pharyngeal epithelium are doubly innervated. Monoamines have been demonstrated in neurones of the nerve net (using an adaptation of the chromaffin method for electron microscopy) while acetylcholinesterase appears to be present in numerous neuromuscular junctions (Karnovksy method; Hernandez-Nicaise, 1976).

Extracellular Recording

Suction electrodes attached to the epithelial surfaces record two classes of events: (*a*) small (<30 μV) biphasic events of regular form and (*b*) larger (<200 μV) irregular multiphasic events. The latter accompany visible ripples of muscular contraction and may be assumed to be compound action potentials from muscle fibers near the surface. The former are presumably nerve net impulses. They closely resemble potentials of nervous origin recorded extracellularly in cnidarian coelenterates (e.g., Mackie, 1975).

FIGURE 2. Small intramesogleal muscle cells. Nomarski optics light micrograph from unfixed undissected piece of body wall. Note the branching of one fiber. Nuclei and/or strands of mitochondria (Mi) are visible in the axis of some fibers. × 800.

FIGURE 3. Cross section of a medium-sized muscle fiber, 18 μm in diameter (transmission electron micrograph). The cell is presumably in a slightly contracted state judging from the few sarcolemmal evaginations (SE) present. (SR) Longitudinal sarcoplasmic reticulum; (Mi) mitochondrion; (N) nucleus. × 11,200.

FIGURE 4. Transverse section of a regular arrangement of thick and thin myofilaments with a number of rosettes present (transmission electron micrograph). × 122,000.

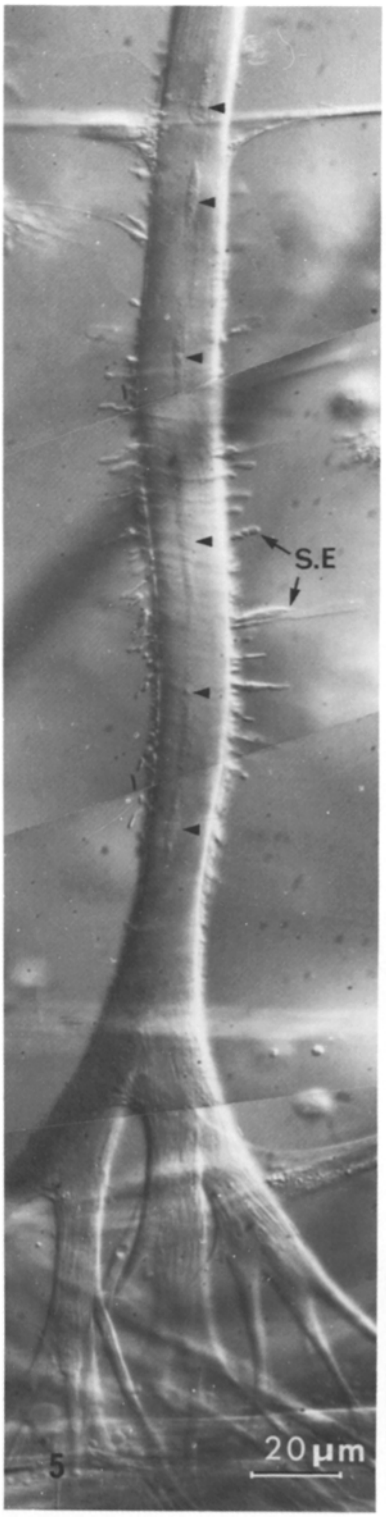
S.E
20 µm
5

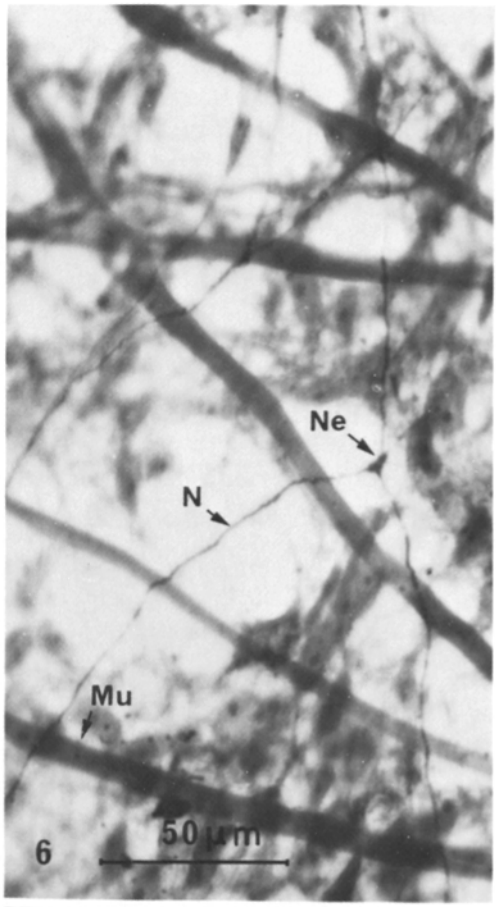
Ne
N
Mu
50 µm
6

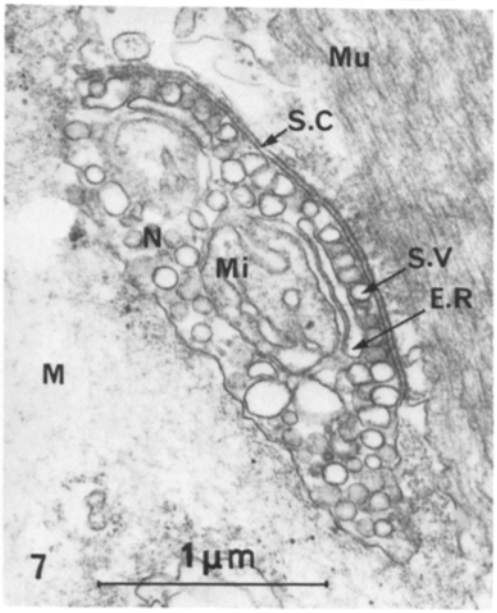
Mu
S.C
N
Mi
S.V
E.R
M
1 µm
7

Single electrical stimuli to the body wall (1–2 ms in duration) were found to evoke the small nervous events singly or in short bursts. These events could be evoked repeatedly, with consistent latencies and wave forms, in both inner (pharyngeal) and outer epithelia (Fig. 8). Conduction for distances of up to 1.5 cm was observed in the pharyngeal epithelium and up to 0.7 cm in the outer. At 22°C, conduction velocities in the range 21–29 cm/s (mean 25 cm/s) were obtained. Nervous conduction across the mesoglea has not been demonstrated.

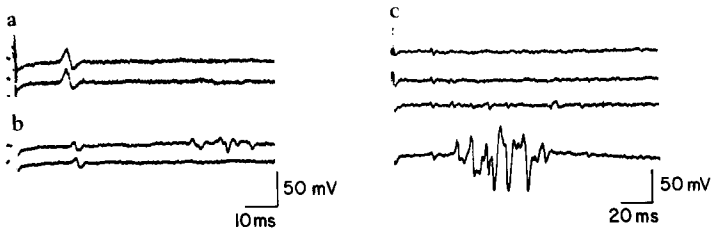

FIGURE 8. Extracellular recordings with suction electrodes attached to the epithelial surfaces. (*a*) Recordings from pharyngeal epithelium, showing presumed nerve net impulses evoked by single, brief (2 ms) electrical stimuli delivered at another point on the same epithelium. The two sweeps show responses to identical stimuli given a few seconds apart without change in recording conditions. (*b*) Outer epithelium, as for *a*. The upper trace includes some spontaneous activity in addition to the evoked impulse. (*c*) Pharyngeal epithelium. The three upper traces were triggered a few seconds apart by identical electrical stimuli. Suction in the recording electrode was increased for the fourth (bottom) trace. The first potential in each trace, and some of the subsequent events, are thought to be nerve net impulses. Muscle potentials are also in evidence and, when recorded at large amplitudes (bottom), tend to mask concurrent nervous activity.

There was considerable background nervous activity consisting of bursts of variable duration. Much of this activity was probably due to stimulation caused by electrodes and pins restraining the animals.

Bursts of nervous activity were often accompanied by muscular contractions but, perhaps because the muscles lie deeper than the nerves, the muscle potentials were usually small and resembled nerve net potentials. Increasing

---

FIGURE 5. The pharyngeal end of a living radial muscle cell: the fiber branches extensively, and the endings anchor upon the epithelium, hidden by the pharyngeal circular muscles. Nomarski interference contrast. Note the multiple nuclei (arrows) and the thin sarcolemmal evaginations (SE). × 600.

FIGURE 6. Intramesogleal nerves running through the mesoglea below the external longitudinal muscles. Ungewitter's silver impregnation. (Mu) Muscle cell; (N) nerve; (Ne) neurone. × 500.

FIGURE 7. Neuromuscular junction (transmission electron micrograph). (ER) Endoplasmic reticulum; (M) mesoglea; (Mi) mitochondrion; (Mu) muscle; (N) nerve; (SC) synaptic cleft; (SV) synaptic vesicle. × 30,000.

the suction on the recording electrode sometimes increased the amplitude of the muscle potentials, presumably by causing the electrode to engulf deeper-lying tissues. In the bottom line of Fig. 8 c there is no muscle potential with the first, directly evoked, nervous event, but a series of muscle potentials of increasing amplitude occurs further on in the record, masking the pattern of nerve events presumed to have triggered it. Such patterns are suggestive of neuromuscular facilitation.

These are the first recordings of nervous events in a ctenophore, but there is already considerable evidence for the involvement of the nerve net in ciliary inhibition, luminescence, and muscle activation (Horridge, 1966; Lábas, 1977 *a*, *b*). Now that nerve net activity can be monitored it should be possible to analyze neuromuscular interactions at the cellular level using micropipettes in the muscle cells. Some preliminary experiments showed evidence of summing junctional potentials in recordings from muscle cells near the epithelial attachment points, but more work is required to substantiate these observations.

Intracellular Recording

USE OF SHORTENED FIBERS One of the potential experimental advantages of *Beroë* muscle fibers is their length which, as has been noted, may be in excess of 6 cm in certain longitudinal fibers. Paradoxically, this extreme length provided one of the major experimental difficulties because of the problem of tracing individual fibers through the body wall. In practice, fibers could be traced in living tissue for no more than 6 mm. Consequently, it was not possible to measure the exact dimensions of individual fibers in a whole animal preparation. Specimens of *Beroë* survive considerable damage, however, and the possibility that the cut ends of the muscle fibers might seal was confirmed as follows: (*a*) Visual observation showed that contraction of injured fibers was restricted to a short damaged region sometimes <1 mm in length. (*b*) A recording from a longitudinal muscle fiber while it separated into two parts showed that the −60 mV resting potential fell to near 0 mV before returning to its previous level within 30 s. (*c*) There was no obvious relationship between the size of the recorded membrane potential and the distance of the recording micropipette from the end of the fiber. (*d*) Except for a region between 1 and 2 mm from a sealed end, action potentials recorded from shortened fibers had the same size and shape as action potentials recorded from a radial muscle which could be seen to cross the body wall from side to side. The prolonged action potentials that were recorded near but not at a sealed end apparently arise because reflections from the end of the fiber arrived back at the recording site in time to delay repolarization (see Fig. 17 *a* and later section). For these reasons it was concluded that work on shortened fibers was justifiable and the following account is confined to studies on such fibers. Note, however, that the shortened fibers were not in most cases spontaneously electrically active, and in view of the lability of spontaneous activity in certain vertebrate smooth muscle tissues, we cannot eliminate the possibility that this is a result of our experimental technique.

EFFECT OF HYALURONIDASE Treatment with hyaluronidase was found to be an effective method of digesting the mesoglea so that muscle cells deep in the body wall could be penetrated with more than one micropipette. Its effect on the membrane properties of *Beroë* muscle cells was tested in a preliminary series of experiments. The results are summarized in Table I. These preliminary findings indicate that there was little difference between the resting potentials of treated and untreated radial fibers, but the average resting potential of enzyme-treated longitudinal fibers was 10 mV more negative than that of the untreated fibers. A possible reason for this difference is that the longitudinal fibers were located deep in the mesoglea and were therefore more likely (than the superficially situated radial fibers) to be damaged during penetration. Another factor is that the radial fibers had, on average, a larger diameter than the longitudinal fibers. This may also account for the 17-mV difference in resting potential between the two groups of untreated fibers. Hyaluronidase had little effect on the average amplitude of

TABLE I
EFFECT OF HYALURONIDASE ON MEMBRANE PROPERTIES OF *Beroë* MUSCLE CELLS

	Longitudinal fibers		Radial fibers	
	Resting potential	Action potential amplitude	Resting potential	Action potential amplitude
	mV		*mV*	
Treated fibers	62±1.3 (n=7)	73±3 (n=7)	68±2 (n=7)	73±2.8 (n=7)
Untreated fibers	52±2 (n=5)	70±1.5 (n=5)	69±3.5 (n=2)	75±3.7 (n=2)

All values are given as means ± SEM.

the action potential (resting potential to overshoot) in either longitudinal or radial muscles. As a consequence, most subsequent experiments (exceptions are indicated) were carried out on hyaluronidase treated preparations.

RESTING POTENTIAL The mean resting potential of a second group of hyaluronidase-treated radial muscle fibers measured in artificial seawater with KCl-filled glass micropipettes was -71 ± 3.5 mV (SE; $n = 8$). This potential is mainly determined by the potassium concentration gradient across the cell membrane. Fig. 9 shows the mean resting potential recorded from radial muscle fibers in this same body wall preparation in different concentrations of external potassium. The graph shows that as predicted from the Nernst equation, the relationship between membrane potential and external potassium was logarithmic over a wide range of concentrations. The straight line was drawn on the assumption that the intracellular potassium concentration was 170 mM. It has a slope of 58 mV for a 10-fold change in the external potassium.

Calcium-free solution on the other hand had very little effect on the resting potential of radial fibers even after prolonged (1–2 h) exposure. The mean resting potential of fibers in calcium-free (magnesium substituted) solution

containing 11 mM potassium was −67 ± 4.7 mV (SE, n = 3). This is in contrast to the effect of low-calcium saline on mammalian smooth muscle which causes a depolarization even when the calcium is replaced by excess magnesium (Bülbring and Kuriyama, 1963; Brading et al. 1969).

ACTION POTENTIAL CHARACTERISTICS AND CONDUCTION VELOCITY From observations on muscle contractions in living *Beroë* and on the basis of the terminal innervation of the muscle fibers, Horridge (1966) suggested that they

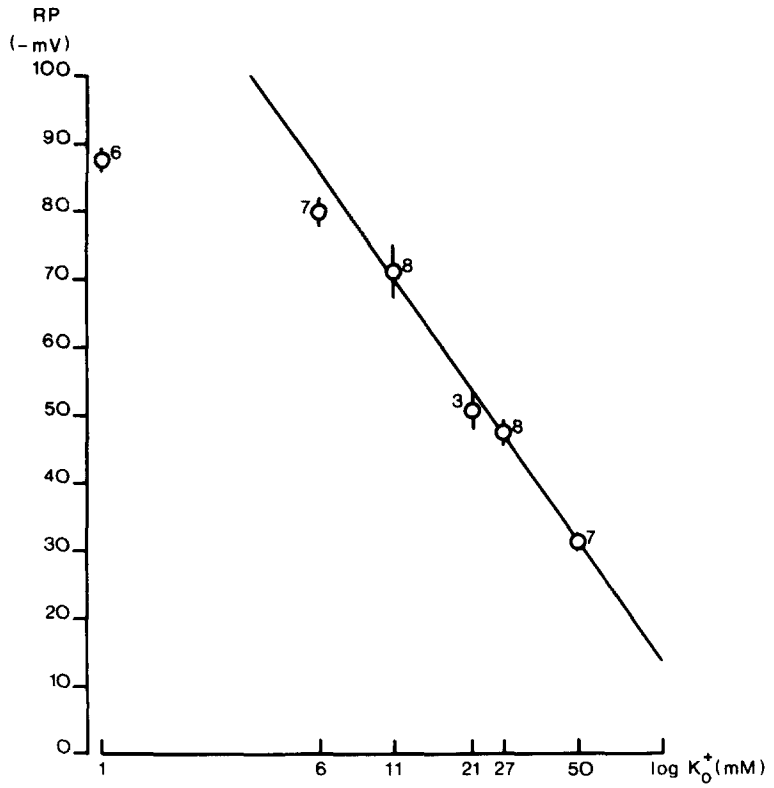

FIGURE 9. The relationship between the membrane potential and the external potassium concentration. The bars give the standard error of the mean; the number of observations is shown. The line drawn through the points has a slope of 58 mV for a 10-fold change in potassium. Potassium was exchanged for sodium.

were capable of impulse propagation. As Fig. 10 shows, this suggestion proved to be correct. The muscle cells were found to be electrically excitable and to produce all-or-none overshooting spikes. The action potential shown in Fig. 10 was recorded intracellularly from two positions along a short length of radial fiber. Its overshoot reaches +27 mV but in other fibers the overshoot was as much as +32 mV (see Fig. 18 *a*). Conduction velocities for this, two other radial fibers, and four longitudinal fibers are shown in Table II.

The conduction velocity of action potentials in excitable cells depends on factors such as fiber diameter and the maximum rate of rise of the action potential. An important question is whether the conduction velocity in *Beroë* fibers is determined by these same factors. Hunter et al. (1975) have provided an analysis of conduction in excitable cells in which the membrane current during a propagated action potential is expressed as a polynomial function of membrane potential. They derive the following relationship between the conduction velocity (θ) and the basic fiber properties.

$$\theta \alpha a^{1/2} R_i^{-1/2} C_m^{-1/2} V_{max}^{1/2} V_p^{1/2}, \quad (1)$$

where a is the fiber radius, R_i is the intracellular resistivity, C_m is the specific capacitance of the membrane, V_{max} is the maximum rate of rise of the action potential, and V_p is the amplitude of the propagated action potential.

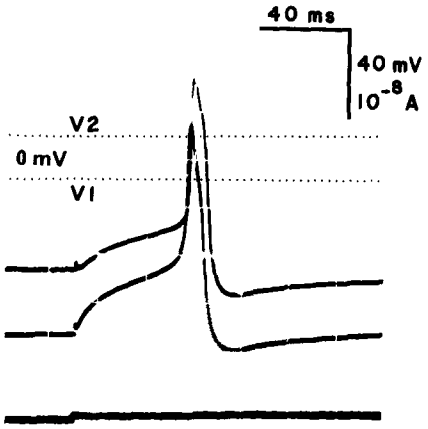

FIGURE 10. Action potential recorded intracellularly at two positions along a short length of radial muscle (total length 1.2 mm). A depolarizing step of current (lower trace) was injected through a third intracellular micropipette which was 0.14 mm from V_1 and 0.99 mm from V_2. The calculated conduction velocity is 59 cm/s. Fiber diameter 35 μm, temperature 21°C. Fiber R-25-D.

Fig. 11, plotted from the data summarized in Table II, shows that, as predicted from Eq. 1, there is a linear relationship between θ^2 and aV_{max}. The slope of this relationship provides a means to estimate C_m. The exact relationship depends on the degree of the polynomial required to describe the current-voltage trajectory. It may be estimated by measuring how far up the rising phase of the action potential the maximum rate of rise occurs (see Hunter et al., 1975). For the action potentials recorded from *Beroë*, the maximum rate of rise is about two-thirds of the way up the action potential. This corresponds to a ninth-degree polynomial and the full expression becomes

$$\theta^2 = 0.93 a V_{max} / C_m R_i V_p. \quad (2)$$

An average value for V_p is 74 mV, and from Fig. 11, $aV_{max}/\theta^2 = 0.15 \times 10^{-4}$

V s/cm. From cable analysis of longitudinal fibers (see Table III) a mean value for R_i is 154 Ωcm. The effective membrane capacitance from Eq. 2 is therefore 1.22 μF.

CABLE PROPERTIES Electrotonic potentials were recorded intracellularly at different distances from a current source (Fig. 12), and it was of interest to discover if the behavior of the fiber could be described by an appropriate cable equation. Because the length of the sealed fibers was no more than 5 mm, it was necessary to use the equation for a short cable (Hodgkin and Nakajima, 1972 *a*):

$$V_m(x, t_\infty) = I_0(r_m r_i)^{1/2}/[\tanh(l_1/\lambda) + \tanh(l_2/\lambda)] \cdot \cosh[(l_2 - x)/\lambda]/\cosh(l_2/\lambda), \quad (3)$$

where V_m is the change in potential difference across the surface membrane, I_0 is the applied current, x is the distance along the fiber from the current

TABLE II

CONDUCTION VELOCITY OF ACTION POTENTIALS RECORDED INTRACELLULARLY FROM *Beroë* MUSCLE CELLS

Fiber	Conduction velocity	Radius	Maximum rate of rise	Action potential amplitude
	cm/s	*μm*	*V/s*	*mV*
L-1-A*	37	13	17	79
L-10-A	47	17	22	78
L-28-B*	29	11	8–16	66
L-28-D	67	14	38	76
R-25-D	59	18	29	80–87
R-25-E	53	12	31	65–77
R-29-D_i	39	17	15–17	62–69
R-29-D_{ii}	68	17	22–27	75

Longitudinal fibers are L-1-A to L-28-D. Radial fibers are R-25-D to R-29-D_{ii}.
* No hyaluronidase used.

source, l_1, l_2 are as defined in Fig. 12, r_1 is the internal resistance of the fiber per unit length, r_m is the membrane resistance × unit length of the fiber, and λ is the length constant of the fiber,

$$\lambda = (r_m/r_i)^{1/2}, \quad (4)$$

t is time, and if V_m is known for two values of x,

$$V_1/V_2 = \cosh[(l_2 - x_1)/\lambda]/\cosh[(l_2 - x_2)/\lambda], \quad (5)$$

λ can be found by trial and error. Then r_m and r_1 can be calculated from Eqs. 3 and 4.

From Hodgkin and Nakajima (1972 *a*) the potential change associated with the make of a constant current in a short fiber is:

$$V_m(X, T) = \tfrac{1}{4} I_0(r_m r_i)^{1/2} \sum_{n=-\infty}^{\infty} \{F[|X + 2n(L_1 + L_2)|, T] + F[|X + 2L_1 + 2n(L_1 + L_2)|, T]\}, \quad (6)$$

where $X = x/\lambda$, $T = t/\tau_m$, $L_1 = l_1/\lambda$, $L_2 = l_2/\lambda$;

$$F(X, T) = e^{-x}\text{erfc}[X/2(T)^{1/2} - T^{1/2}] - e^{x}\text{erfc}[X/2(T)^{1/2} + T^{1/2}], \quad (7)$$

n is equivalent to the number of reflections from the ends of the fiber, $n = -\infty, \ldots -2, -1, 0, 1, 2, \ldots \infty$, and τ_m is the time constant of the membrane.

In the present case it was unnecessary to consider that the current was reflected from the ends of the fiber more than once. Hence:

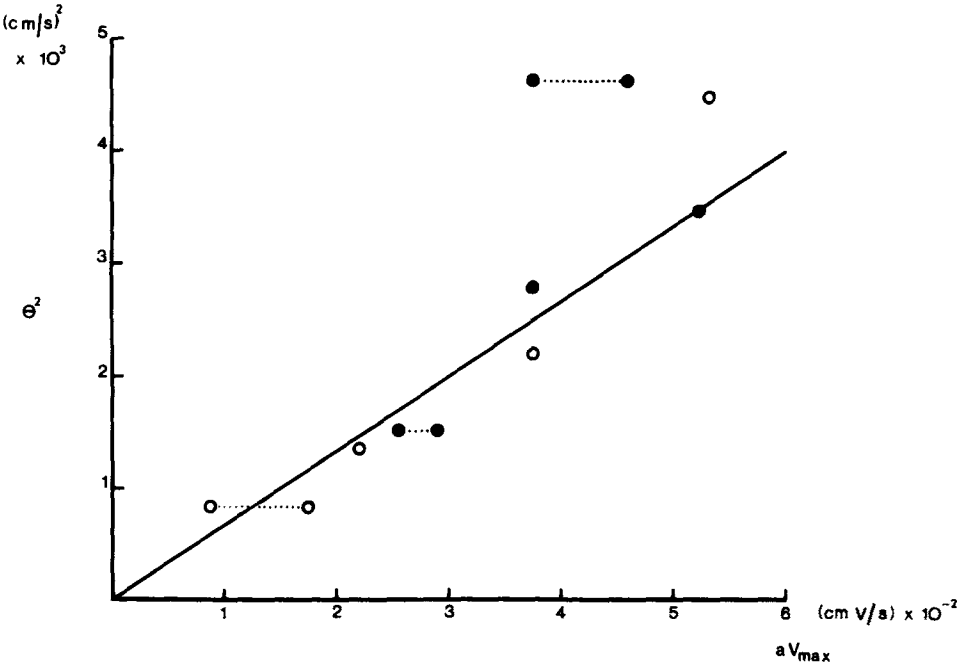

FIGURE 11. Relationship between θ^2 and aV_{max}. The data is summarized in Table II. (●) Radial muscles, (○) longitudinal muscles. The line indicates the average slope with fiber R-29-D_{ii} excluded. The slope aV_{max}/θ^2 becomes 0.13 $\times 10^{-4}$ V s/cm if R-29-D_{ii} is included, and the effective capacitance is then 1.1 μF.

$$V_m(X, T) \doteq \tfrac{1}{4}[I_0(r_m r_i)^{1/2}]\{F(X, T) + F(X + 2L_1, T) + F(X + 2L_1 + 2L_2, T) + F(X + 4L_1 + 2L_2, T) + F(-X + 2L_1 + 2L_2, T) + F(-X + 2L_2, T)\}. \quad (8)$$

A table of F at different values of X and T is given by Hodgkin and Rushton (1946) and this was used to evaluate the different terms of the equation.

Table III summarizes the results obtained from five longitudinal fibers. Radial muscles are not suitable for analysis because of their branching ends. R_i, the specific resistivity of the interior of the fiber $= \pi a^2 r_i$. The resistance of the surface membrane × unit area $(R_m) = 2\pi a r_m$. The time constant of the membrane (τ_m) was measured by fitting $V_m(X, T)$ calculated from Eq. 8 to

the experimental record at $T = 1$. The apparent membrane capacity per unit area at low frequency (C'_m) was calculated from $C'_m = \tau_m/R_m$.

As noted above, it is difficult to trace these fibers for distances longer than about 6 mm in unfixed preparations and hence an infinite cable model is not

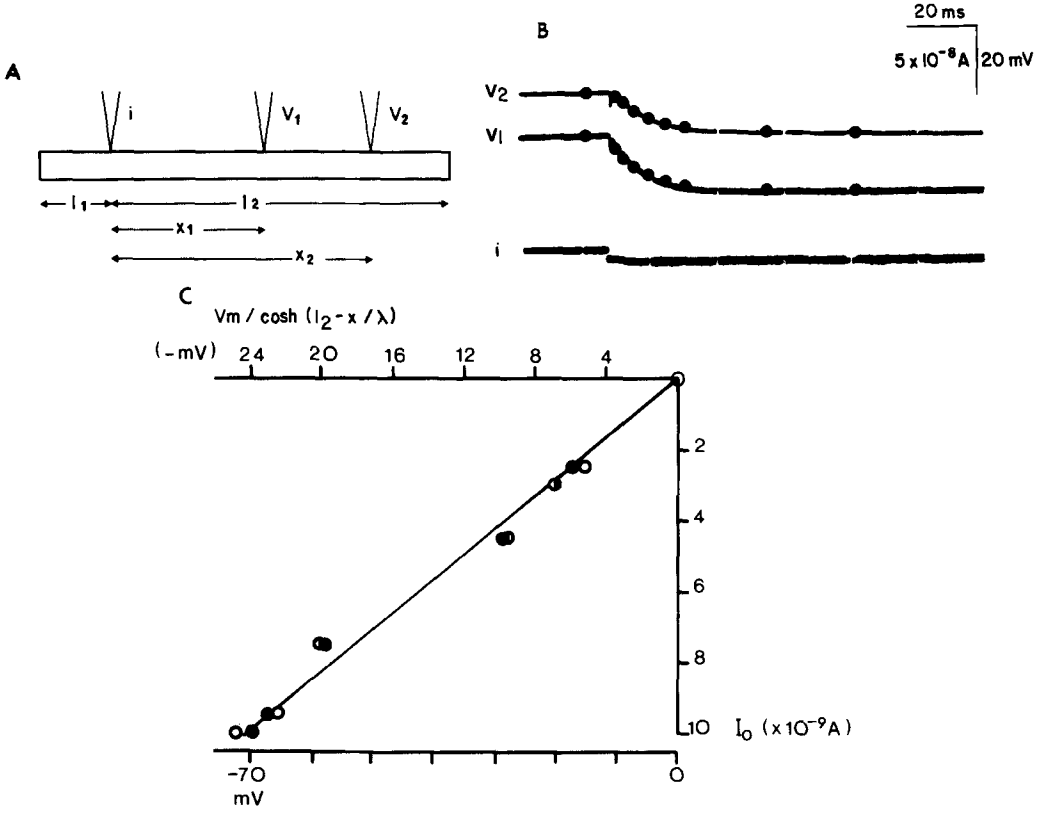

FIGURE 12. Arrangement of micropipettes for analysis of a short cable with sealed ends. V_1 and V_2 are intracellular recording micropipettes; i is for current injection. (B) Records of membrane potential change recorded intracellularly at two positions along a longitudinal muscle in response to an injected current step of 5.6×10^{-9} A. The current source was 0.22 mm from V_1 (middle trace) and 1.05 mm from V_2 (top trace). (●) Points calculated from Eq. 8; $l_1 = 0.55$ mm; $l_2 = 2.15$ mm; $\lambda = 1.95$ mm; $\tau_m = 11.8$ ms; fiber diameter 27 μm. Fiber L-28-D. (C) Relationship between injected current (I_0) and $V_m/\cosh(l_2-x/\lambda)$. (●) $x = 0.57$ mm; (○) $x = 2$ mm. The lower abscissa gives the calculated change in membrane potential at the point of current injection, i.e., $x = 0$; $l_2 = 3.33$ mm; $\lambda = 1.92$ mm; fiber diameter 22 μm. Fiber L-28-B.

strictly applicable. However, on one occasion a single longitudinal fiber (*L*-1-*B*) known to be longer than 6 mm was penetrated at different distances from a current source with a recording micropipette. The fiber was treated as a leaky cable of infinite length and the membrane constants calculated are shown in Table III. The values for λ, R_i, and R_m obtained were in agreement with values obtained using the equation for a short cable.

In Fig. 12 B, the membrane potential response to the make of a constant current is shown recorded at two points along the fiber from the current source. The solid circles show V_m at different values of T calculated from Eq. 8 and are a good fit to the experimental record.

Fig. 12 C is taken from the results of an experiment on another fiber. It shows that a graph of $V_m/\cosh(l_2 - x/\lambda)$ against I_0 is approximately linear over a wide range of membrane potential in the hyperpolarizing direction and for both positions of the recording electrode. The graph is readily converted into a plot of membrane potential at $x = 0$ against injected current. From Eq. 3 the slope of the line gives

$$(r_m r_i)^{1/2}/[\tanh(l_1/\lambda) + \tanh(l_2/\lambda)]\cosh l_2/\lambda,$$

from which r_i and r_m may be calculated.

TABLE III

ELECTRICAL CONSTANTS OF *Beroë* LONGITUDINAL MUSCLES

Fiber	Radius	Length	λ	R_i	R_m	τ_m	C'_m
	μm	mm	mm	Ωcm	Ωcm²	ms	μF/cm²
L-24-C	9	2.7	1.95	118	9,900	14.3	1.4
L-26-B	23	4.9	2.4	213	19,900	—	—
L-28-B*	11	3.5	1.92	140	9,300	15.7	1.7
L-28-C	9	2.1	1.55	193	10,300	—	—
L-28-D	14	2.7	1.95	108	5.867	11.8	2.0
Mean±SEM			1.95 ±0.1	154 ±21	9,253 ±886	13.9 ±1.1	1.7 ±.2
L-1-B	10	>6	1.7	140	7,300	—	—

* No hyaluronidase used.

The mean membrane resistance of *Beroë* muscles referred to fiber surface was about 9,000 Ωcm². Some caution in making comparison with other tissues is necessary because of the effect of potassium and the membrane potential on membrane resistance (Jenerick, 1953). The membrane resistance of different axons in seawater is comparable to that of the *Beroë* muscles. It averages about 8,000 Ωcm² in crab (Hodgkin, 1947) and may be up to 7,330 Ωcm² in lobster (Hodgkin and Rushton, 1946). It can be 5,400 Ωcm² or more in squid (Cole 1968) although the nominally accepted value is 1,000 Ωcm² (Cole and Hodgkin, 1939). The resistance of the surface membrane of frog fast skeletal muscle is also about 9,000 Ωcm² (from Hodgkin and Nakajima, 1972 *a*), although the bathing medium is rather different. This is lower than the value for frog slow muscle (29,000 Ωcm², Adrian and Peachey, 1965) and for guinea-pig taenia coli (30,000–60,000 Ωcm², Tomita, 1970).

The mean apparent membrane capacity at low frequency of *Beroë* muscles was found to be 1.7 μF/cm². This is in agreement with a calculated value of 1.7 μF/cm² for guinea-pig taenia coli (if τ_m is 106.7 ms, λ is 1.45 mm, and the longitudinal tissue impedance is 300 Ωcm; Abe and Tomita, 1968; Tomita, 1970) and of 1.6 μF/cm² for the slow fibers of the frog iliofibularis muscle

(Adrian and Peachey, 1965). The value is comparable to the surface membrane capacity of frog skeletal muscle (1 $\mu F/cm^2$, Hodgkin and Nakajima, 1972 *b*) and other membranes (Curtis and Cole, 1938; Hodgkin and Rushton, 1946; Hodgkin, 1947).

Although the estimate of membrane capacitance and resistance for *Beroë* muscle is comparable to that of other excitable tissues, the mean value of R_i (154 Ωcm at 20–22°C in artificial seawater) is higher than that found for other marine organisms. This is true for either muscle fibers (crab, 69 Ωcm, Fatt and Katz, 1953) or for nerve axons (lobster, 60.5 Ωcm, Hodgkin and Rushton, 1946; crab, 90 Ωcm, Hodgkin, 1947; squid 35.4 Ωcm, Hodgkin and Huxley, 1952) and cannot be entirely attributed to the errors inherent in optical measurements of fiber diameter through the mesoglea (estimated to be ±10%). The value is, however, close to that of 170 Ωcm found for isolated frog skeletal muscle fibers at the same temperature (Hodgkin and Nakajima, 1972 *a*). In guinea-pig taenia coli the sarcoplasmic resistivity is also 100–200 Ωcm (Tomita, 1970).

IONIC MECHANISM OF THE ACTION POTENTIAL Action potentials may be recorded from *Beroë* muscle fibers in salines deficient in either sodium or calcium ions, but not in saline deficient in both sodium and calcium. Fig. 13 shows that full-sized action potentials may be recorded after 30 min exposure to a saline in which $CaCl_2$ had been replaced by $MgCl_2$. The effect of 30 min exposure to a saline containing the normal concentration of calcium (10 mM) but only 25 mM sodium (NaCl replaced by an isosmotic equivalent of Tris/Tris-HCl) is shown in Fig. 14 *a*. There is no evidence for restricted diffusion through the mesoglea because action potentials recorded within 10 min of changing the bathing medium to one nominally free of Ca^{++} and containing 25 mM Na^+ were small and graded (see Fig. 14 *b*; sodium and calcium were replaced as above). These graded action potentials were found to be absent if $MnCl_2$ was added to the medium (Fig. 14 *d*). However, full-sized action potentials could be recorded after 30 min in artificial seawater containing freshly prepared $CoCl_2$ (35 mM; Fig. 16 *b*) or $MnCl_2$ (25 mM; not illustrated), agents known to suppress calcium currents in other tissues. These results suggest that whereas calcium ions contribute little to the action potentials under normal conditions, they may be an important component of the inward current in sodium-deficient medium. This conclusion is confirmed by the observation that action potentials recorded in sodium-deficient solution were blocked within 60 s of adding 25 mM $CoCl_2$ (Fig. 15). Clearly, the hyaluronidase-treated preparation provided little barrier to diffusion. It may be that under normal conditions, sodium ions may be important simply because seawater contains 50 times as much sodium as calcium.

EFFECT OF TETRODOTOXIN Sodium currents in many but not all (see Moreton, 1972; Wald, 1972) excitable tissues are blocked by tetrodotoxin (TTX). Full-sized action potentials were recorded from *Beroë* muscles even after 1–2 h exposure to artificial seawater containing 10^{-5} g/ml TTX or after similar treatment with a calcium-free TTX saline (not illustrated). In this respect then *Beroë* muscles resemble vertebrate smooth muscle (Tomita, 1975).

EFFECT OF VERAPAMIL Verapamil is considered to be a potent inhibitor of calcium-dependent action potentials, and in vertebrate smooth muscle, both action potentials and contractions are blocked by 5×10^{-6} g/ml (Golenhofen and Lammel, 1972). In *Beroë* muscle fibers low concentrations of verapamil (2×10^{-6} g/ml) were without apparent effect on the action potential even after 30 min exposure (Fig. 16 *a*); but the effect of verapamil

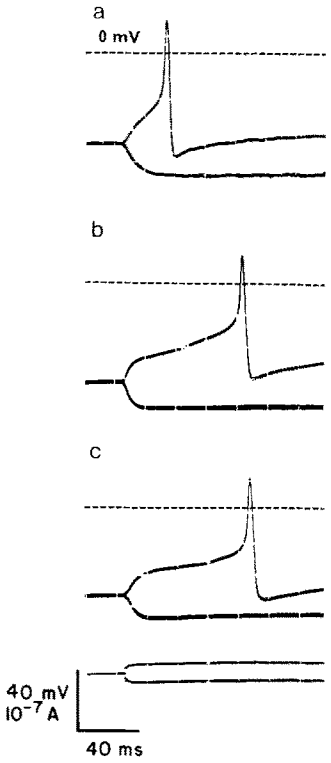

FIGURE 13. The effect of calcium-free saline on action potentials recorded from radial muscle fibers. Records from same piece of body wall but from different fibers: (*a*) normal saline; (*b*) after 30 min in calcium-free saline, calcium replaced by magnesium; (*c*) after return to normal saline. Each record shows the effect of hyperpolarizing and depolarizing current pulses, traces superimposed. The injected current is shown at the bottom of the figure.

in low sodium-containing solutions was not tested. Higher concentrations had the effect of inducing violent contractions in previously quiescent preparations, an effect which has also been reported in crayfish muscles (Suarez-Kurtz and Sorenson, 1977). In *Beroë* the induced contractions were abolished by calcium-free saline.

As shown in Fig. 17 (traces I–III), the immediate effect of 6×10^{-5} g/ml verapamil on the *Beroë* action potential was to increase the overshoot, reduce

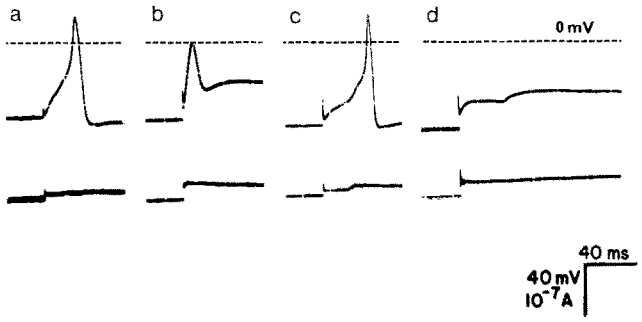

FIGURE 14. Action potentials recorded from radial muscle: (*a*) in 25 mM Na^+ (Tris) saline (after 30 min); (*b*) in 25 mM Na^+, 0 mM Ca^{++} saline (after 10 min); (*c*) in normal saline 5 min after (*a*) and (*b*); (*d*) in 25 mM Na^+, 0 mM Ca^{++} saline, containing 25 mM $MnCl_2$ (after 10 min). Lower traces indicate injected current.

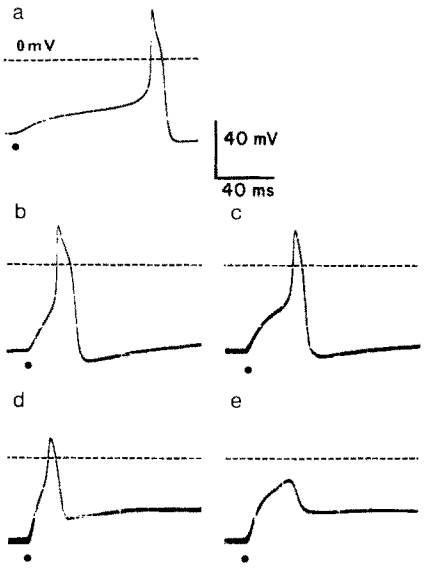

FIGURE 15. Effect of cobalt chloride on action potentials recorded from longitudinal muscle fibers in low-sodium saline. Action potentials from fiber in (*a*) normal saline; (*b*) 25 mM Na^+ (Tris) saline after 30 min; (*c*) 25 mM Na^+ saline 10 s after addition of 25 mM $CoCl_2$; (*d*) same after 20 s; (*e*) same after 30 s. (*b–e*) Action potentials recorded successively from same fiber. Action potentials resulted from a step depolarization established at the black spot.

the rate of rise and prolong the falling phase. The undershoot was also decreased. This was followed within minutes by a considerable reduction of the overshoot and a further increase in duration (traces IV–VII, Fig. 17). In this particular experiment the fiber was preconditioned with a hyperpolarizing current pulse in order to oppose the possible depolarizing effects of the verapamil.

The initial increase in duration of the action potential in Fig. 17 may result at least partly from the reduction in its conduction velocity associated with the decrease in the rate of rise. This would have the effect of delaying the current reflected from the end of the fiber. The increase in overshoot may indicate a genuine reduction in outward current which could account for the reduced undershoot. Verapamil appears to reduce delayed rectification in both cardiac Purkinje fibers (Cranefield et al., 1974; Rosen et al., 1974) and in the x-organ neurone of the crayfish (Kuroda, 1976). An effect of 10^{-4} g/ml verapamil on the sodium-dependent action potential (in 10 mM $MnCl_2$) recorded from the x-organ has also been reported (Kuroda, 1976). In guinea-pig ureter, the sodium-dependent plateau phase is reduced (Shuba, 1977). These effects may be analagous to that observed on *Beroë* action potentials.

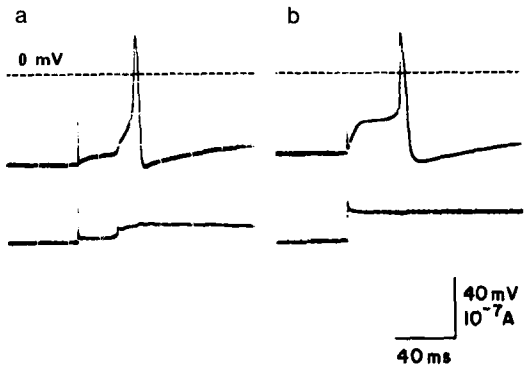

FIGURE 16. (*a*) Effect of 2×10^{-6} M verapamil on action potential recorded from radial muscle fiber after 15 min. (*b*) Effect of 35 mM cobalt chloride on action potential recorded from longitudinal muscle fiber after 30 min. Lower traces indicate injected current.

EFFECT OF LOW-POTASSIUM SALINE AND OF TETRAETHYLAMMONIUM IONS The effect of low-K^+ saline is shown in Fig. 18 *b*. Although the resting potential is more negative, there is no comparable increase in the action potential undershoot. Furthermore, the action potential remained unaffected by 50 mM tetraethylammonium chloride (TEA) added to the bathing medium even after 30 min exposure (Fig. 18 *c*). The effect of injecting TEA was not tested. It is possible that potassium activation plays only a minor role in the repolarization of the membrane during an action potential.

PROLONGED ACTION POTENTIALS Action potentials of normal duration (~5 ms) could be recorded close to a sealed end of a shortened fiber, but in a region between 1 and 2 mm removed, the action potentials were considerably prolonged (see Fig. 17 *a*). It is unlikely that the plateau was because of fiber damage. The duration of the plateau (~10 ms) is consistent with the hypothesis that the plateau represents a decremental reflection of the conducted action potential from the sealed ends of the fiber. In the experiment shown in Fig. 17 *a*, the recording site and current source were 0.5 mm apart, and each was 1 mm from one end to the fiber and 1.5 mm from the other. The fiber diameter

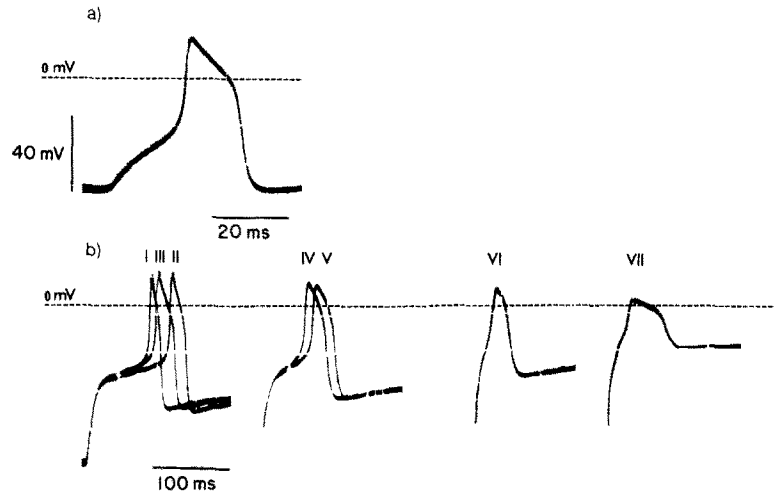

FIGURE 17. Effect of 6×10^{-5} g/ml verapamil on action potential recorded from a longitudinal muscle fiber. (*a*) Action potential recorded from fiber in normal saline. (*b*) Successive action potentials recorded (I) before and (II) 15 s, (III) 30 s, (IV) 2 min, (V) 2.5 min, (VI) 3 min, and (VII) 5 min after addition of 6×10^{-5} g/ml iproveratril to the bathing medium. Action potentials in *b* followed a 200-ms hyperpolarizing current pulse (2×10^{-8}A).

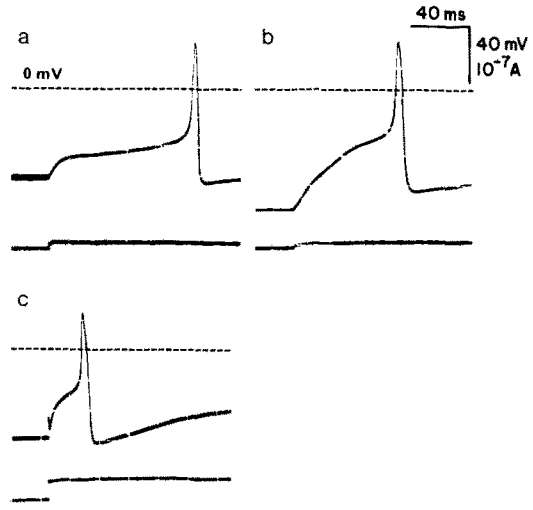

FIGURE 18. Action potentials recorded from radial muscle fibers; (*a*) in normal saline; (*b*) in 1 mM K^+ saline; (*c*) in normal saline plus 50 mM tetraethylammonium chloride. Lower traces indicate injected current.

was 27 μm, the maximum rate of rise of the action potential was 25 V/s and so the conduction velocity should be about 48 cm/s (see Fig. 11). The conduction velocity of the reflected decremental wave is unknown because it depends largely on the resistance of the cell membrane. In a fiber treated as

an infinite cable (Hodgkin and Rushton, 1946) it should be ~28 cm/s ($2\lambda/\tau_m$; see Table III). Assuming that this approximates to the true value, the wave reflected from one end should return in 5.7 ms while that reflected from the other should arrive 0.75 ms later. It is possible that waves such as these could sum to produce the prolonged action potential observed, but if so, it means that the membrane resistance during the repolarizing phase of the action potential must be relatively high.

DISCUSSION

The mesogleal muscles of ctenophores have a number of features that make them particularly suitable for electrophysiological research. The muscles are arranged in layers of large cylindrical fibers which run freely within the transparent mesogleal matrix. There is a wide separation of individual fibers, which is probably not related to any marked ability for independent action on the part of single fibers but may be an adaptation allowing the fibers access to nutrients diffusing through the mesoglea and serving to distribute tensional changes evenly within the soft body of the animal. Whatever the functional significance of this pattern, it is of an advantage from an electrophysiological point of view because it allows single fibers to be visualized and recorded from with relative ease. The main problem with using this preparation, however, arises from the arrangement of the longitudinal fibers. They overlap each other in such a fashion as to make it difficult to trace an individual fiber in vivo for a distance greater than about 5–6 mm. Another difficulty is to stabilize the preparation in order to maintain one or more micropipettes in a single fiber for any length of time. Much of the movement arises from the spontaneous contractions of small muscle fibers under the pharangeal epithelial surface. In order to stabilize the preparation as much as possible, it is necessary to strip away much of this surface. For these reasons a whole animal preparation is at present impracticable. Although the shortened fibers used in this investigation fail to make full use of the extreme length of the longitudinal fibers, we believe that in the future it should be possible to isolate lengths of several centimeters by enzymatic digestion.

An experimental advantage revealed by this study is that these muscle fibers have relatively little infolding of the surface membrane. Electrophysiological analysis of relaxed fibers shows that the membrane capacity is relatively low at both low and higher frequencies. Fibers with smooth surfaces are seen in unfixed preparations under Nomaski interference contrast. In many sections of tissue fixed for electronmicroscopy, however, the cell periphery shows large evaginations which, by analogy with similar profiles observed in mammalian smooth muscles (Fay and Delise, 1973; Fay et al., 1976), probably result from folding during contraction. In these fibers, the surface area calculated from the diameter underestimates the true membrane surface by a factor of three or more.

The basic ultrastructural features of *Beroë* muscle cells resemble the general features of mammalian smooth muscles. In particular, the ultrastructure and spatial arrangement of the myofilaments have many points in common (Somlyo and Somlyo, 1975). However, there are at least two basic important

differences that set these *Beroë* cells apart: (*a*) there are no anchoring dense structures for the thin microfilaments that we suppose to be attached to the sarcolemma; (*b*) no junctions have been observed between the reticulum and the surface membrane.

In spite of the insensitivity to tetrodotoxin, there are also clear differences in the electrophysiology of *Beroë* fibers when compared with vertebrate smooth muscle. It is difficult to generalize because of the differences among animals and among different tissues in the same animal. For example, (*a*) sodium-free saline blocks action potentials in rat myometrium (Anderson et al., 1971; Kao and McCullough, 1975) whereas action potentials in guinea-pig taenia coli (Brading et al., 1969) and myometrium (Vassort, 1976) appear to be independent of sodium; (*b*) TEA increases the amplitude of the action potential in the myometrium of estradiol-treated guinea-pigs (Vassort, 1975) but not in the estrogen-dominated rat myometrium (Anderson and Ramon, 1976); (*c*) the amplitude and rate of rise of action potentials recorded from guinea-pig taenia coli are increased by a conditioning hyperpolarization (Kuriyama and Tomita, 1965), whereas in the myometrium of both guinea-pig and rat, conditioning hyperpolarization reduces the net inward currents (Anderson and Ramon, 1976; Kao and McCullough, 1975; Vassort, 1975). Nevertheless, action potentials in all three of these tissues are blocked by 1–2 mM manganese chloride and in general, agents known to suppress calcium currents are more effective on vertebrate smooth muscle than they are on *Beroë* muscle.

If as seems likely, calcium ions trigger contraction in *Beroë* smooth muscles, influx of calcium across the surface membrane may be necessary for contractile activation. There is little to suggest intracellular release of calcium; the sarcoplasmic reticulum has a relatively low volume, and as we have noted, junctions between the reticulum and surface membrane were not observed. However, neither is there any discernable contraction associated with an action potential even in sodium-deficient saline. This raises questions about the ionic basis of the large stretch induced contractions which are the most obvious mechanical activity of these cells.

APPENDIX

Hunter et al. (1975) have provided an analysis of conduction in excitable cells in which the membrane current during a propagated action potential is expressed as a polynomial function of membrane potential. In the above account we have used this treatment to estimate the specific capacitance of the membrane of *Beroë* muscle cells. Here we provide evidence that the method is a reliable one. We have used previously published data for guinea-pig taenia coli (Tomita, 1966; Fig. 3, p. 223), frog sartorius and semitendinosus muscles (Hodgkin and Nakajima, 1972 *b*; Fig. 1 A, C and Table I), and squid giant axon (Hodgkin and Huxley, 1952, Fig. 15 C and p. 528) to calculate C_m from Eqs. 1 and 2. Table IV shows the relevant data and the values calculated. The values of C_m in brackets are for comparison. They are taken from the original authors. In the case of the muscle fibers they were calculated from the time-course of the foot of the action potential. In the case of the squid axon the value shown was measured according to the methods of Hodgkin et al. (1952).

TABLE IV

SPECIFIC MEMBRANE CAPACITANCE CALCULATED FROM MEASUREMENTS TAKEN FROM PROPAGATED ACTION POTENTIALS RECORDED INTRACELLULARLY IN DIFFERENT EXCITABLE TISSUES

Fiber	θ	a	R_i	V_{max}	V_p	Degree polynomial	Calculated C_m
	cm/s	*μm*	*Ωcm*	*V/s*	*mV*		*μF*
1. Guinea-pig taenia coli (35°C)	7	2	300*	11	75	13	1.67 (1.13)
2. Frog sartorius (3.6°C) Wh-2-F	57	42	284‡	104	122	7	4.11 (3.72)
3. Frog semitendinosus (22.5°C) Bd-29-C	254	70	169	507	124	9	2.44 (2.75)
4. Squid giant axon (18.5°C)	2,120	238	35.4	559	95	7	0.93 (1.0)

Data sources:

1. Tomita, 1966, Fig. 3, p. 223.
2,3. Hodgkin and Nakajima, 1972 *b*, Fig. 1 A, C and Table I.
4. Hodgkin and Huxley, 1952, p. 528 and Fig. 15 C.

Note: values of C_m in parentheses are from original author's calculations (see text).

* Longitudinal tissue impedance, the sum of R_i and junctional resistance (Tomita, 1970).

‡ Calculated using $Q_{10} = 1.37$ (Hodgkin and Nakajima, 1972 *a*).

The authors wish to express their thanks to the Director and staff of the Station Zoologique, Université Pierre et Marie Curie, Villefranche-sur-Mer for their hospitality during the course of this work, and to Dr. Peter McNaughton and Dr. Oger Rougier for their comments on the manuscript.

The work was supported by grants from the Centre National de la Recherche Scientifique de la France (Laboratoire Associé No. 244) to Dr. Hernandez-Nicaise, from the National Research Council of Canada to Dr. Mackie (No. A1427), and from the Browne Fund of the Royal Society to Dr. Meech.

Received for publication 19 March 1979.

REFERENCES

ABE, Y., and T. TOMITA. 1968. Cable properties of smooth muscle. *J. Physiol. (Lond.)*. **196**:87–100.

ADRIAN, R. H., and L. D. PEACHEY. 1965. The membrane capacity of frog twitch and slow muscle fibres. *J. Physiol. (Lond.)*. **181**:324–336.

ANDERSON, N. C., and F. RAMON. 1976. Interaction between pacemaker electrical behavior and action potential mechanism in uterine smooth muscle *In* Physiology of Smooth Muscle. E. Bülbring and M. F. Shuba, editors. Raven Press, New York. 53–63.

ANDERSON, N. C., F. RAMON, and A. SNYDER. 1971. Studies on calcium and sodium in uterine smooth muscle excitation under current-clamp and voltage-clamp conditions. *J. Gen. Physiol.* **58**:322–339.

BRADING, A., E. BÜLBRING, and T. TOMITA. 1969. The effect of sodium and calcium on the action potential of the smooth muscle of the guinea-pig taenia coli. *J. Physiol. (Lond.)*. **200**: 637–654.

BÜLBRING, E., and H. KURIYAMA. 1963. Effects of changes in the external sodium and calcium concentrations on spontaneous electrical activity in smooth muscle of guinea-pig taenia coli. *J. Physiol. (Lond.)*. **166**:29–58.

COLE, K. S. 1968. Membranes, ions and impulses. University of California Press, Berkeley and Los Angeles. 73–76.

COLE, K. S., and A. L. HODGKIN. 1939. Membrane and protoplasm resistance in the squid giant axon. *J. Gen. Physiol.* **22**:671–687.

CRANEFIELD, P. F., R. S. ARONSON, and A. L. WIT. 1974. Effect of verapamil on the normal action potential and on a calcium-dependent slow response of canine cardiac purkinje fibers. *Circ. Res.* **34**:204–213.

CURTIS, H. J. and K. S. COLE. 1938. Transverse electric impedance of the squid giant axon. *J. Gen. Physiol.* **21**:757–765.

DEVINE, C. E., A. V. SOMLYO, and A. P. SOMLYO. 1972. Sarcoplasmic reticulum and excitation-contraction coupling in mammalian smooth muscles. *J. Cell Biol.* **52**:690–718.

FATT, P., AND B. KATZ. 1953. The electrical properties of crustacean muscle fibres. *J. Physiol. (Lond.).* **120**:171–204.

FAY, F. S., P. H. COOKE, and P. G. CANADAY. 1976. Contractile properties of isolated smooth muscle cells. *In* Physiology of Smooth Muscles. E. Bülbring and M. F. Shuba, editors. Raven Press, New York. 249–264.

FAY, F. S., and C. M. DELISE. 1973. Contraction of isolated smooth-muscle cells—structural changes. *Proc. Natl. Acad. Sci. U. S. A.* **70**:641–645.

FRANC, J. M. 1970. Evolutions et interactions tissulaires au cours de la régénération des lèvres de *Beroë ovata* (Chamisso et Eysenhardt), Cténaire Nudicténide. *Cah. Biol. Mar.* **11**:57–76.

GABELLA, G. 1973. Fine structure of smooth muscle. I. Cellular structures and electrophysiological behaviour. *Philos. Trans. R. Soc. London B. Biol. Sci.* **265**:7–16.

GOLENHOFEN, K., and E. LAMMEL. 1972. Selective suppression of some components of spontaneous activity in various types of smooth muscle by iproveratril (verapamil). *Pflügers. Arch. Eur. J. Physiol.*, **331**:233–243.

HERNANDEZ-NICAISE, M-L. 1973 *a*. Le système nerveux des cténaires. I. Structure et ultrastructure des réseaux épithéliaux. *Z. Zellforsch. Mikrosk. Anat.* **137**:223–250.

HERNANDEZ-NICAISE, M-L. 1973 *b*. Le système nerveux des cténaires. II. Les éléments nerveux intra-mésogléens des béroidés et des cydippidés. *Z. Zellforsch. Mikrosk. Anat.* **143**:117–133.

HERNANDEZ-NICAISE, M-L. 1973 *c*. The nervous system of Ctenophora. III. Ultrastructure of synapses. *J. Neurocytol.* **2**:249–263.

HERNANDEZ-NICAISE, M-L. 1976. Evidence for neural control of muscles in Ctenophores. *In* Coelenterate Ecology and Behavior. G. O. Mackie, editor. Plenum Press, New York. 513–522.

HERTWIG, R. 1880. Über den Bau der Ctenophoren. *Jena. Z. Naturwiss.* **14**:393–457.

HODGKIN, A. L. 1947. The membrane resistance of a non-medullated nerve fibre. *J. Physiol. (Lond.).* **106**:305–318.

HODGKIN, A. L., and A. F. HUXLEY. 1952. A quantative description of membrane current and its application to conduction and excitation in nerve. *J. Physiol. (Lond.).* **117**:500–544.

HODGKIN, A. L., A. F. HUXLEY, and B. KATZ. 1952. Measurement of current-voltage relations in the membrane of the giant axon of *Loligo. J. Physiol. (Lond.).* **116**:424–448.

HODGKIN, A. L., and S. NAKAJIMA. 1972 *a*. The effect of diameter on the electrical constants of frog skeletal muscle fibres. *J. Physiol. (Lond.).* **221**:105–120.

HODGKIN, A. L., and S. NAKAJIMA. 1972 *b*. Analysis of the membrane capacity in frog muscle. *J. Physiol. (Lond.).* **221**:121–136.

HODGKIN, A. L., and W. A. H. RUSHTON. 1946. The electrical constants of a crustacean nerve fibre. *Proc. R. Soc. Lond. B. Biol. Sci.* **133**:444–479.

HORRIDGE, G. A. 1966. Pathways of coordination in Ctenophores. *In* The Cnidaria and their Evolution. W. J. Reese, editor. Academic Press, Inc., London. 247–266.

HUNTER, P. J., P. A. MCNAUGHTON, and D. NOBLE. 1975. Analytical models of propagation in excitable cells. *Prog. Biophys. Mol. Biol.* **30:**99–144.

JENERICK, H. P. 1953. Muscle membrane potential, resistance, and external potassium chloride. *J. Cell. Comp. Physiol.* **42:**427–448.

KAO, C. Y., and J. R. MCCULLOUGH. 1975. Ionic currents in the uterine smooth muscle. *J. Physiol. (Lond.).* **246:**1–36.

KURIYAMA, H., and T. TOMITA. 1965. The responses of single smooth muscle cells of guinea-pig taenia coli to intracellularly applied currents, and their effect on the spontaneous electrical activity. *J. Physiol. (Lond.).* **178:**270–289.

KURODA, T. 1976. The effects of D600 and verapamil on action potential in the x-organ neuron of the crayfish. *Jpn. J. Physiol.* **26:**189–202.

LÁBAS, Y. A. 1977 *a*. Triggering and regulatory mechanisms of the ciliary beating in Ctenophora. I. Coordination of ciliary beating with intracellular bioluminescence and muscle contractions. *Tsitologiya.* **19:**514–521.

LÁBAS, Y. A. 1977 *b*. Triggering and regulatory mechanisms of the ciliary motion in the ctenophore *Bolinopsis*. II. Effect of ionic changes on the ciliary apparatus and bioluminescence system of a Ctenophore *Tsitologiya.* **19:**644–654.

MACKIE, G. O. 1975. Neurobiology of *Stomotoca*. II. Pacemakers and conduction pathways. *J. Neurobiol.* **6:**357–378.

MORETON, R. B. 1972. Electrophysiology and ionic movements in the central nervous system of the snail, *Helix aspersa*. *J. Exp. Biol.* **57:**513–541.

ROSEN, M. R., J. P. ILVENTO, H. GELBAND, and C. MERKER. 1974. Effects of verapamil on electrophysiological properties of canine cardiac Purkinje fibers. *J. Pharmacol. Exp. Ther.* **189:** 414–422.

SHUBA, M. F. 1977. The effect of sodium-free and potassium-free solutions, ionic current inhibitors and ouabain on electrophysiological properties of smooth muscle of guinea-pig ureter. *J. Physiol. (Lond.).* **264:**837–851.

SOMLYO, A. P., and A. V. SOMLYO. 1975. Ultrastructure of smooth muscle. *Methods Pharmacol.* **3:**3–43.

SUAREZ-KURTZ, G., and A. L. SORENSON. 1977. Effects of verapamil on excitation-contraction coupling in single crab muscle fibers. *Pflügers Arch. Eur. J. Physiol.* **368:**231–239.

TOMITA, T. 1966. Membrane capacity and resistance of mammalian smooth muscle. *J. Theor. Biol.* **12:**216–227.

TOMITA, T. 1970. Electrical properties of mammalian smooth muscle. *In* Smooth Muscle. E. Bülbring, A. F. Brading, A. W. Jones, and T. Tomita, editors. Edward Arnold, London. 197–243.

TOMITA, T. 1975. Electrophysiology of mammalian smooth muscle. *Prog. Biophys. Mol. Biol.* **30:** 185–203.

VASSORT, G. 1975. Voltage-clamp analysis of transmembrane ionic currents in guinea-pig myometrium: evidence for an initial potassium activation triggered by calcium influx. *J. Physiol. (Lond.).* **252:**713–734.

VASSORT, G. 1976. Transmembrane ionic currents in guinea pig myometrium during excitation. *In* Physiology of Smooth Muscle. E. Bülbring and M. F. Shuba editors. Raven Press, New York. 77–81.

WALD, F. 1972. Ionic differences between somatic and axonal action potentials in snail giant neurones. *J. Physiol. (Lond.).* **220:**267–281.